Journal Pre-proof

Graphite modified sodium alginate hydrogel composite for efficient removal of malachite green dye

Ankit Verma, Sourbh Thakur, Gcina Mamba, Prateek, Raju Kumar Gupta, Pankaj Thakur, Vijay Kumar Thakur

Please cite this article as: A. Verma, S. Thakur, G. Mamba, et al., Graphite modified sodium alginate hydrogel composite for efficient removal of malachite green dye, *International Journal of Biological Macromolecules*(2020), https://doi.org/10.1016/j.ijbiomac.2020.01.142

This is a PDF file of an article that has undergone enhancements after acceptance, such as the addition of a cover page and metadata, and formatting for readability, but it is not yet the definitive version of record. This version will undergo additional copyediting, typesetting and review before it is published in its final form, but we are providing this version to give early visibility of the article. Please note that, during the production process, errors may be discovered which could affect the content, and all legal disclaimers that apply to the journal pertain.

Graphite modified sodium alginate hydrogel composite for efficient removal of malachite green dye

Ankit Verma[a], Sourbh Thakur[a,b*], Gcina Mamba[c], Prateek[d], Raju Kumar Gupta[d,e], Pankaj Thakur[a,f] and Vijay Kumar Thakur[g,h*]

[a]School of Chemistry, Faculty of Basic Sciences, Shoolini University, Solan, 173229, Himachal Pradesh, India

[b]Center for Computational Materials Science, Institute of Physics, Slovak Academy of Sciences, 84511 Bratislava, Slovakia

[c]Nanotechnology and Water Sustainability Research Unit, College of Science, Engineering and Technology, University of South Africa, Florida 1709, Johannesburg, South Africa

[d]Department of Chemical Engineering, Indian Institute of Technology Kanpur, Kanpur, 208016, UP, India

[e]Center for Environmental Science and Engineering, Indian Institute of Technology Kanpur, Kanpur 208016, Uttar Pradesh, India

[f]Department of Environmental Sciences, Central University of Himachal Pradesh, Shahpur, Dist. Kangra, Himachal Pradesh-176206

[g]Enhanced Composites and Structures Center, School of Aerospace, Transport and Manufacturing, Cranfield University, Bedfordshire MK43 0AL, UK

[h]Department of Mechanical Engineering, School of Engineering, Shiv Nadar University, Uttar Pradesh, 201314, India

Abstract

Herein, porous sodium alginate/graphite based hybrid hydrogel was fabricated as an effective adsorbent for organic pollutant. Sodium alginate was modified through graft polymerisation of acrylic acid and subsequently loaded with graphite powder to enhance its adsorption capability. The synthesized sodium alginate cross-linked acrylic acid/graphite (NaA-cl-AAc/GP) hydrogel composite was utilized in the removal of malachite green (MG) dye from aqueous solution using batch adsorption experiments. The NaA-cl-AAc/GP hydrogel composite was characterized by infrared spectroscopy, raman spectroscopy, thermo-gravimetric analysis, scanning electron microscopy, x-ray photoelectron spectroscopy and x-ray diffraction. Under optimized experimental conditions, a maximum adsorption capacity of 628.93 mg g^{-1} was attained for malachite green dye. Moreover, the adsorption process could be well described by the langmuir isotherm model and pseudo-second-order kinetic model. The hydrogel composite also showed 91% adsorption after three consecutive cycles of dye adsorption-desorption. Therefore, the NaA-cl-AAc/GP hydrogel composite is a potentially favourable material towards dye pollution remediation owing to its better swelling rate, environment friendliness, high adsorption potential and regeneration capability.

***Corresponding authors Email: thakursourbh@gmail.com, vijay.kumar@cranfield.ac.uk

1. Introduction

Over the years, water pollution remediation has attracted global attention due to the continuous deterioration of the water quality as a result of the invasion by organic, inorganic and microbial pollutants [1]. Water is a potentially useful resource therefore availability of water is important for the continued existence of living things on earth. However, large quantities of pollutants are directly or indirectly introduced into freshwater water bodies

where they render the water unsafe for day to day use [2,3]. Hydrogel based water purification systems have shown the potential as efficient adsorbents because of their three-dimensional network of polymeric chains and hydrophilic nature [4]. Moreover, hydrogel materials are more advantageous because they are cheap, non-toxic, chemically and physically stable, have a flexible polymeric network and good reusability [4,5]. The flexible polymeric network supports the swelling property of the hydrogel enabling it to hold a considerable amount of water without dissolving [6]. Many chemical and physical methods like adsorption, chemical oxidation and reduction, biological treatment and photocatalytic degradation have been used for wastewater remediation [7]. However, the adsorption method is a favourable physical method for wastewater treatment owing to its cost-effectiveness and environmental friendliness, among other advantages [8].

Sodium alginate (NaA) is a pH sensitive, non-toxic, biodegradable, natural, anionic polymer formed of two basic units: α-L-guluronic acid (G-block) and β-D-mannuronic acid (M-block) [9,10]. Alginate has been mainly used in the pharmaceutical, medical and food industries, therefore alginate based adsorbents in water treatment have shown pronounced concern by reason of their biocompatibility and non-toxic nature [11–13].

Graphite has a 3D layered structure of graphene sheets stacked together and held by weak van der Waals forces and is often used as the source material for other modified carbon forms including graphene, graphene oxide, reduced graphene oxide and graphite oxide [14–16]. Graphite and its derivatives show good chemical properties, thermal stability and mechanical strength. So these properties of graphite making it an ideal material for improving the stability of hydrogel composite [17,18]. *He et al*., synthesized yttrium/graphene oxide/sodium alginate hydrogels by sol-gel method and utilized for the removal of fluoride [19]. *Bradder et al.,* prepared graphite oxide for the surface assimilation of dye particles from aqueous solution [20]. In another work, *Fan et al.,* synthesized a graphene oxide based hydrogel for

the removal of cationic and anionic dye pollutants [18]. These studies have demonstrated the positive effect of incorporating the carbon materials in the hydrogel composite for adsorption of various pollutants.

Malachite green dye is an organic cationic dye **(Figure S1)** that is widely used in the textile and paper industries [21,22]. Generally, the removal of organic dyes from aqueous solutions is a great challenge [23,24]. Malachite green dye has been highlighted as one of the causes of high heartbeat, headache, and irritation of the eyes [25,26]. Therefore, its efficient removal from wastewater is of priority.

In recent time, many research works have been performed for removal of MG dye from aqueous solution by using hydrogel composite. Hosseinzadeh and Sonia Ramin, prepared the starch-graft-poly(acrylamide)/graphene oxide/hydroxyapatite hydrogel nanocomposite for removal of MG dye. The maximum adsorption capacity of the hydrogel composite for MG dye was examined to 297 mg g^{-1} [14]. Similarly, a magnetic bacterial cellulose nanofiber/graphene oxide polymer aerogel was synthesized by Payam Arabkhani and Arash Asfaram for adsorption of MG dye with maximum adsorption tendency of 270.27 mg g^{-1} [27]. These types of research works demonstrated the capability of hydrogel nanocomposites in detoxifying water laden with organic pollutants. But, in present work, we have synthesized the sodium alginate and graphite hydrogel composite for MG dye removal with high adsorption capacity of 628.93 mg g^{-1}. The synthesized hydrogel composite shows exceptional high adsorption capacity in comparison to previously reported adsorbents.

Herein, we performed hot air oven-assisted synthesis of hydrogel composite by free radical polymerization of sodium alginate, acrylic acid and graphite powder. The prepared sodium alginate cross-linked acrylic acid/graphite powder (NaA-cl-AAc-GP) hydrogel composite was used as an absorbent to remove malachite green dye from aqueous solutions. Also, we

discussed the effect of various reaction conditions such as pH, adsorbent dose, dye concentration and contact time on dye adsorption behaviour of the hydrogel composite. Reaction kinetics and adsorption isotherm models were employed to study the adsorption behaviour of the dye on the prepared adsorbent.

2. Experimental

2.1 Materials

Sodium alginate (NaA), $C_6H_9NaO_7$ (MW = 216.12 g mol^{-1}) with low viscosity, acrylic acid (AAc), $C_3H_4O_2$ (MW = 72.06 g mol^{-1}), potassium per sulphate, 98% (KSO), $K_2S_2O_8$ (MW = 270.31 g mol^{-1}) and graphite fine powder 98% (GP) (MW = 12.01 g mol^{-1}) were purchased from LOBA CHEMIE PVT. LTD., India. N,N'-methylene bis-acrylamide (MBA), $C_7H_{10}N_2O_2$ (MW = 154.17 g mol^{-1}) was purchased from SD Fine-Chem limited India. Malachite green (MG) dye was purchased from CENTRAL DRUG HOUSE (CDH) PVT. LTD., India. Double distilled water was used for the preparation of samples. All chemicals were of analytical grade and were used without further purification. The pH of the solutions were adjusted by 0.1N NaOH and 0.1N HCl solution. Details of experimental section are provided in supplementary information. Schematic representation of the preparation route and photographs of the hydrogel composite are shown in the **Scheme 1**.
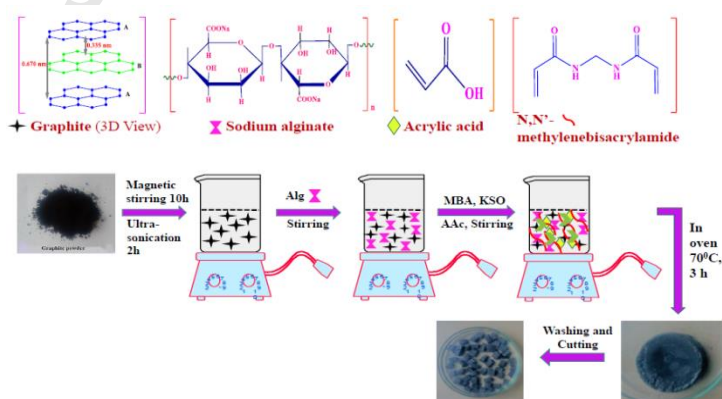
Scheme 1. Schematic representation for the synthesis of the NaA-cl-AAc-GP hydrogel composite.

2.2. Analysis of point zero charge (pzc)

For pzc analysis, 50 mL of distilled water was taken in a 150 mL conical flask. The pH of water was adjusted between 2 to 11 using 0.1N NaOH and 0.1N HCl solutions. Around 0.5 g of sample was added to the pH solution and then kept under shaking (rpm-90) for 24 hours to catch the equilibrium point. After 24 hour, pH of the liquid was measured denoted as pH_f. The value of pzc for prepared sample was evaluating by plotting a graph between initial pH (pH_i) against difference between initial (pH_i) and final pH (pH_f).

3. Result and discussion

A proposed mechanism for the chemical cross-linking of sodium alginate with acrylic acid and graphite is presented in **scheme 2a**. Firstly, the initiator KSO decomposed under heating to produce sulphate ion radicals. These sulphate ions then react with water to form OH radicals, which further react with the NaA polymeric backbone and monomer to generate active free radical sites. Subsequently, AAc grafted onto the NaA backbone and form long polymeric chains. Meanwhile, the cross-linker linked the long polymeric chains to form three dimensional NaA-cl-AAc-GP hydrogel composite. **Scheme 2b** show the possible interaction between the polymeric matrix and graphite. Mainly three types of possible interactions are represented in the scheme: covalent bonding, electrostatic interaction and π-π interactions [28].
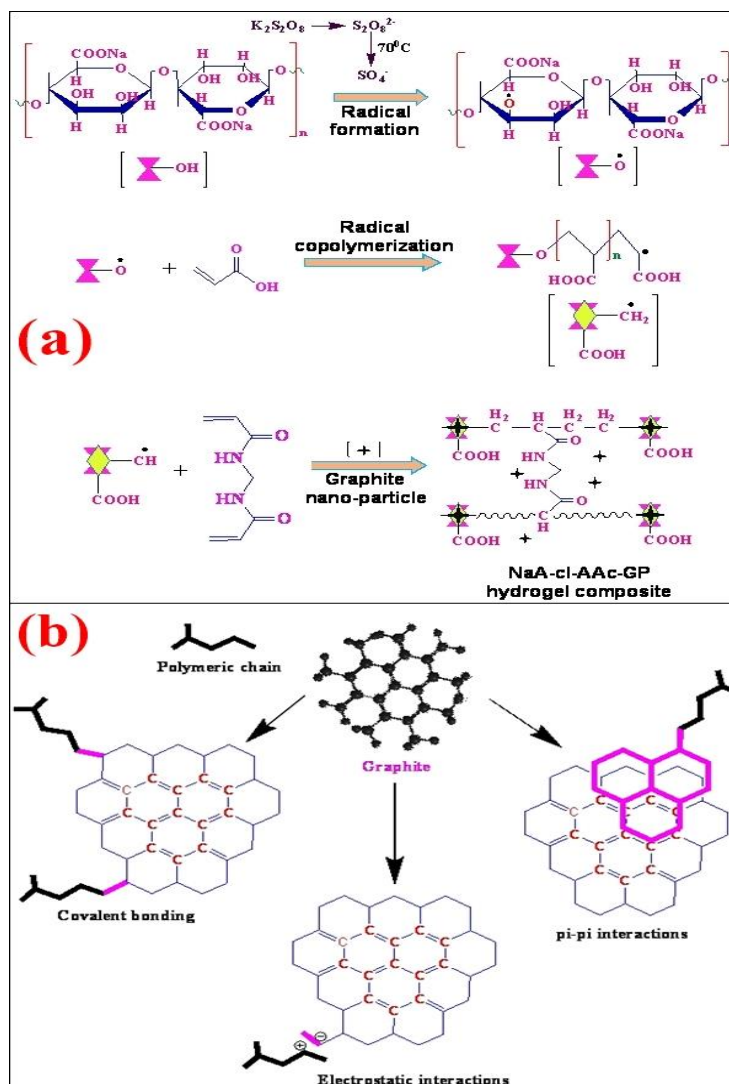
Scheme 2. (a) The proposed chemical mechanism for the synthesis of NaA-cl-AAc-GP hydrogel composite and (b) possible interactions between polymeric chain and graphite.

3.1. Swelling study

3.1.1. Effect of GP concentration on hydrogel composite swelling

The swelling percentage of the hydrogel composite increased with GP concentration (**Figure S2**), reaching a maximum swelling capacity of 3838.65 % when 0.050 g of GP was incorporated. However, beyond 0.050 g, the excess GP ruptures the three-dimensional structure of the composite, which resulted in a decrease in swelling capacity. Moreover, the excess GP resulted in a decrease in the hydrophilicity of the hydrogel composite, resulting in poor interaction with water.

3.2. Point zero charge of prepared hydrogel composite

The adsorption of MG dye depends on the electrostatic interaction between the functional groups of the dye molecule and surface functionality of the hydrogel composite. The surface charge of hydrogel composite varies with the change in initial pH of water. With the increase in pH_i, the functional groups of hydrogel composite undergo deprotonation. In detail, the hydrogel's surface will be positively charged if $pH_i < pH_{pzc}$ and it will be negatively charged if $pH_i > pH_{pzc}$. In our analysis, the pH_{pzc} for hydrogel composite is 6.5, which means for pH values below 6.5 (**Figure 1**), the active sites on hydrogel composite are positively charged and are not favorable for the adsorption of cationic MG dye. At pH values of higher than 6.5, the surface of the hydrogel composite are negatively charged. Conclusively, the hydrogel composite shows negative surface charge at pH 7.
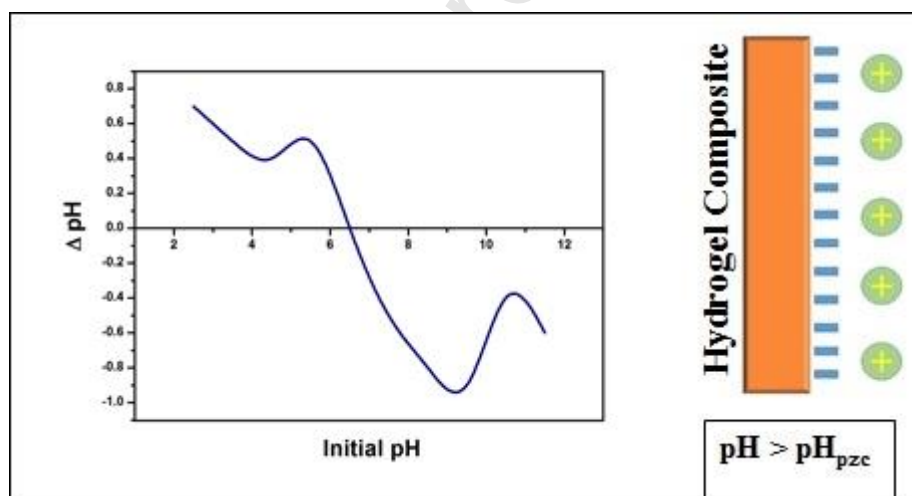

Figure 1. The point zero charge graph for hydrogel composite.

3.3. Fourier transform infrared spectroscopy (FTIR)

The FTIR spectrum of NaA, NaA-cl-AAc hydrogel andNaA-cl-AAc-GP hydrogel composite are represented in **Figure 2.** In the spectra of sodium alginate, a broad peak at 1030 cm^{-1} emanates from the stretching of C-O group. The presence of the arabinosyl functionality was verified by the presence of a sharp peak at 1102 cm^{-1} while the other sharp peaks at 879 cm^{-1}

and 873 cm^{-1} are attributed to the β-glycosidic linkage between the mannuronic and guluronic units of NaA[29]. Meanwhile, the broad peaks at 2931 cm^{-1} and 1406 cm^{-1} were due to the sp^3 C-H asymmetric stretching mode and the C-C bending vibration, respectively. The broad peaks at 3434 cm^{-1} and 1030 cm^{-1} are due to the stretching vibration of hydroxyl and C-O-C groups [12,30]. After polymerization of sodium alginate with acrylic acid, an additional peak appeared at 1722 cm^{-1}, confirming the grafting of the monomer onto the NaA backbone [31–33]. The peaks at 813 cm^{-1} and 812 cm^{-1} are characteristic of the Na-O stretching in the NaA and NaA-cl-AAc spectra while the sharp peak at 1632 cm^{-1} is assigned to symmetric and asymmetric vibrations of the COO$^-$ groups. Decrease in intensity and broadness of the peaks 3434 cm^{-1} and 1406 cm^{-1} are attributed to the incorporation of GP in the NaA-cl-AAc hydrogel. Disappearance of the peaks at 873 cm^{-1} and 813 cm^{-1} may be due to the addition of GP in the hydrogel matrix. After adsorption of MG dye on the NaA-cl-AAc-GP hydrogel composite, peak at 1711 cm^{-1} due to carboxylic groups are almost disappeared **(Figure S3)** and broadness/intensity of the peaks at 3434 cm^{-1} and 2922 cm^{-1} are goes down. The subsequent changes in the peaks confirm that MG dye adsorbed in the NaA-cl-AAc-GP hydrogel composite.
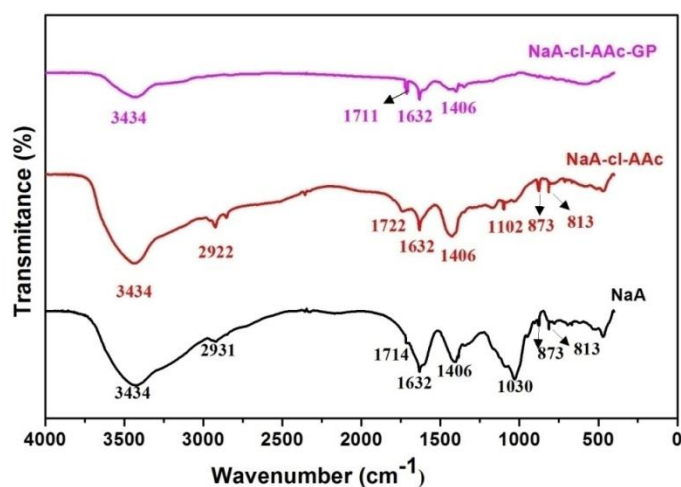

Figure 2. FTIR spectra of NaA, NaA-cl-AAc hydrogel and NaA-cl-AAc-GP hydrogel composite.

3.4. X-ray photoelectron spectroscopy (XPS)

Qualitative chemical analysis was performed by XPS and the wide scan XPS spectra of NaA, NaA-cl-AAc, GP and NaA-cl-AAc-GP hydrogel composite is presented in **Figure 3a**. In particular, the survey scan of NaA-cl-AAc and NaA-cl-AAc-GP hydrogel composite shows the presence of the elements C and O while only C was identified in GP and Na was detected in addition to C and O in the case of NaA. Upon deconvolution of the C1s high resolution spectrum of NaA-cl-AAc-GP (**Figure 3b**), two peaks with binding energies at 282.9 and 286.1 eV corresponds to the C-C and C=O groups, respectively [34]. Meanwhile, the O1s high resolution spectrum was deconvoluted into two peaks at 530.2 and 531.1 eV **(Figure 3c)** which could be assigned to O from C=O and C-O, respectively [35]. **Figure S4a** shows the high resolution XPS of C1s, O1s and Na1s orbitals for pure NaA. The orbital spectrum of Na1s region has two major peaks at 1070 eV and 1069 eV, confirming the presence of sodium in two forms: ionic sodium and sodium oxide [36]. The Auger peak (Na KLL) at 495.7 eV indicated the presence of elemental sodium on the surface of NaA [37]. After the crosslinking of NaA with AAc new peaks were introduced in the C1s orbital at 287 eV due to the C-O-C and C-OH (**Figure S4b**). In case of GP, the fitted spectra for C1s region shows peaks at 282.2 and 282.5 eV attributed to C-C rings (**Figure S4c**) [38,39]. After the adsorption of MG dye on hydrogel composite, the intensity of peak at 287 eV is decreased in the C1s spectra **(Figure S4d)**. In O1s spectra, broadness of peaks at 531 eV and 530 eV also confirm the MG dye adsorption on NaA-cl-AAc-GP hydrogel composite **(Figure S4d)**.
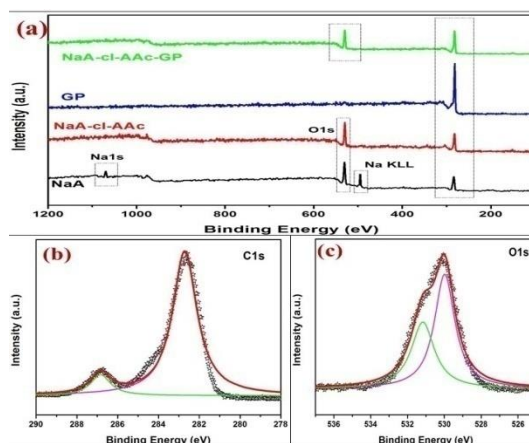
Figure 3. XPS spectra for all pure and prepared samples (a) combined spectra, (b) NaA-cl-AAc-GP hydrogel composite for C1s and (c) NaA-cl-AAc-GP hydrogel composite for O1s.

3.5. X-ray diffraction (XRD)

Figure 4 shows the XRD patterns of NaA, NaA-cl-AAc hydrogel, GP and NaA-cl-AAc-GP hydrogel composite. The XRD pattern of NaA is characteristic of the amorphous nature of the material with two broad peaks at 13.61° and 21.5° corresponding to the (110) and (200) crystal planes of guluronic and mannuronic units, respectively [40]. Subsequent to grafting, there was a decrease in the diffraction peak intensity and enhancement in broadening of the NaA-cl-AAc hydrogel peaks, which suggested successful grafting of AAc onto the NaA backbone. On the other hand, the XRD pattern of GP showed an intense, sharp peak at 26.6° corresponding to the (002) diffraction plane of graphene layers [41] and another smaller peak at 54.2° corresponding to the (004) diffraction plane of GP [42]. The incorporation of GP into the NaA-cl-AAc hydrogel matrix was clearly confirmed by the appearance of the two characteristic GP peaks at 26.6° and 54.2°, as shown in the XRD pattern of NaA-cl-AAc-GP hydrogel composite. The two peaks 26.6° and 54.2° are visible in the spectra of MG loaded NaA-cl-AAc-GP hydrogel composite but intensity of the peaks were decreased due to adsorption of MG dye **(Figure S5)**. Moreover, the entrapped dye molecules led to the increase in isotropic behaviour of the hydrogel structure.
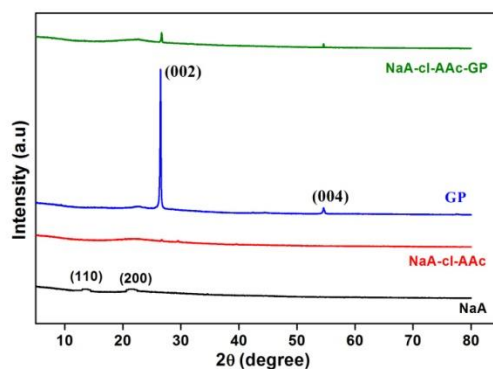
Figure 4. XRD spectrum of NaA, NaA-cl-AAc hydrogel, GP and NaA-cl-AAc-GP hydrogel composite.

3.6. Thermal analysis

TGA analysis was performed to gain information about the thermal stability of the NaA, NaA-cl-AAc hydrogel, GP, and NaA-cl-AAc-GP hydrogel composite (**Figure S6**). The initial mass losses in the temperature range 30-145 °C which were 14.9 %, 6.7 % and 4.3% for NaA, NaA-cl-AAc hydrogel and NaA-cl-AAc-GP hydrogel composite could be assigned to the loss of adsorbed moisture. On the other hand, the major mass losses in NaA (43.6%), NaA-cl-AAc hydrogel (44%) and NaA-cl-AAc-GP hydrogel composite (41.9%) occurring between 165-298 °C were due to the breaking of glycosidic bonds and dehydration of the polysaccharide rings. The final mass losses from 355 to 530° C for NaA-cl-AAc hydrogel (22.9 %) and NaA-cl-AAc-GP hydrogel composite (10.6 %) were due to the decomposition of cross-linked polymeric chain. Most importantly, the TGA analysis clearly confirmed that NaA-cl-AAc-GP hydrogel composite was more thermally stable compared to the NaA and NaA-cl-AAc hydrogel due to the incorporation of the highly stable GP particles. The DTG spectra of NaA, NaA-cl-AAc hydrogel, GP and NaA-cl-AAc-GP hydrogel composite are shown in **Figure S7**. From the derivatives of the mass loss spectra, it could be seen that the decomposition temperature was at 67.46 °C and 249.65 °C for NaA, 224.49 °C, 248.66 °C and 391.84 °C for NaA-cl-AAc hydrogel and 262.98 °C and 401.57°C for NaA-cl-AAc-GP

hydrogel composite. Conclusively, the decomposition temperatures of NaA-cl-AAc hydrogel are less than those of the NaA-cl-AAc-GP hydrogel composite, indicating a positive influence of GP on thermal stability of the composite.

3.7. Raman spectroscopy analysis

The Raman spectra for GP and NaA-cl-AAc-GP hydrogel composite are shown in **Figure 5**. In the GP spectrum, two pecks were observed at 1336 cm^{-1} and 1560 cm^{-1}, corresponding to the disordered (D-band) and graphitic peaks (G-band) of GP, respectively [43,44]. The disordered peak confirmed the disruption of either the edges or topological defects in the graphite sheets and the amount of disorder in the graphite sheets is directly related to the D band intensity. In addition, the presence of the G band confirms the symmetric sp^2 C-C bonds stretching (1560 cm^{-1}) [45]. In the spectrum of NaA-cl-AAc-GP hydrogel composite, the emergence of the D band (1336 cm^{-1}) and G band (1560 cm^{-1}) confirmed the successful incorporation of graphite in the hydrogel. Moreover, an additional peak at 2702 cm^{-1} was indicative of graphite exfoliation due to stirring and sonication of graphite powder. The disappearance of peak at 2702 cm^{-1} and increased in broadness of peaks at G (1570 cm^{-1}) and D (1346 cm^{-1}) bands assigned to the adsorption of malachite dye molecules on the NaA-cl-AAc-GP hydrogel composite **(Figure S8)**.
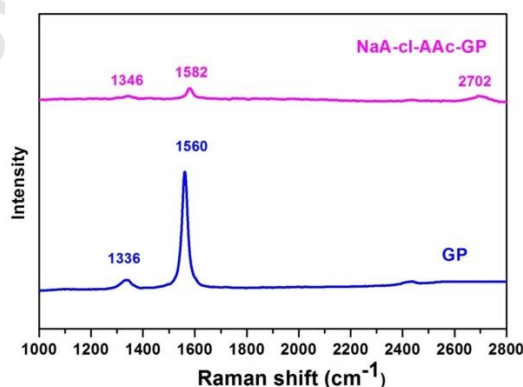

Figure 5. Raman spectra for GP and NaA-cl-AAc-GP hydrogel composite.

3.8. Morphology analysis

FESEM analysis was used to examine the morphology of NaA-cl-AAc-GP hydrogel composite (**Figure 6**). Sodium alginate (NaA) had a smooth and flat surface **(Figure S9a,b)** but after grafting with acrylic acid, the surface became rough **(Figure S9c,d)**. FESEM images of GP show its sheet-like nature, with relatively smooth and uniform surfaces (**Figure S9e,f**). After the incorporation of GP, there was formation of interconnected filamentous structures within the hydrogel matrix (**Figure 9a,b**). This filamentous network covers the interconnected pores of the NaA-cl-AAc-GP hydrogel composite from inside to the outside. This could be linked to the stacked graphene layers of GP. After dye adsorption, the surface morphology of hydrogel composite becomes utterly different from the unloaded hydrogel composite. The surface of dye-loaded hydrogel composite seems to be smoother which is probably due to the voids filled by the dye molecules (**Figure S9g,h**).
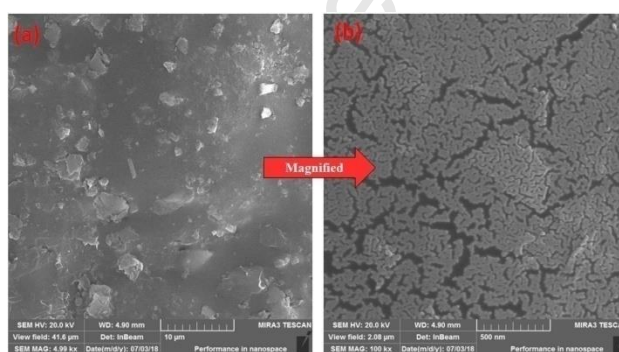

Figure 6. The FESEM images of prepared NaA-cl-AAc-GP hydrogel composite.

4. Adsorption of MG dye by NaA-cl-AAc-GP hydrogel composite

The prepared NaA-cl-AAc-GP hydrogel composite was investigated for the removal of toxic organic dye from aqueous solution. A possible mechanism for interaction between NaA-cl-AAc-GP hydrogel composite and organic dye (MG) is represented in **Scheme 3**.
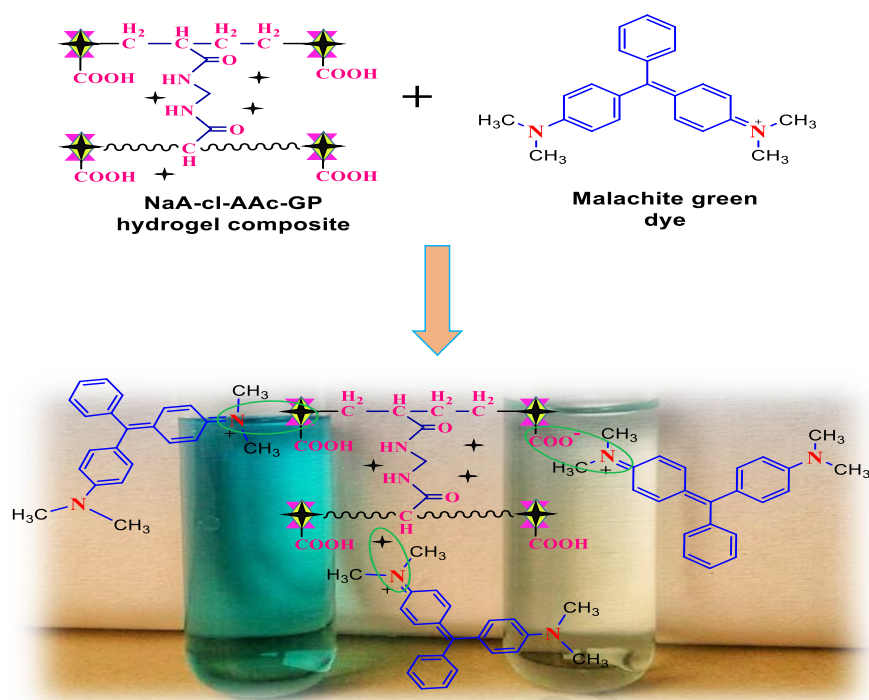
Scheme 3. Possible mechanism for the interaction between hydrogel composite and MG dye.

Due to the differences in surface charge, electrostatic interactions arise between the carboxylic group (COO⁻) of NaA-cl-AAc-GP hydrogel composite and MG dye. Moreover, hydrogen bonding between MG dye and hydroxyl ions of the sodium alginate sub-units play an important role in ensuring efficient interaction. In addition, the presence of GP in the NaA-cl-AAc-GP hydrogel composite increases the affinity of the hydrogel composite towards MG dye due to potentially negative surface of GP, which further increases the electrostatic attractions between the cationic (MG) dye and negatively charged adsorbent. Hence, coupling of GP with NaA-cl-AAc hydrogel in an adsorbent seem more satisfactory adsorbent than using pure GP and NaA-cl-AAc hydrogel, individually.

4.1. Effect of GP loading on MG adsorption

The amount GP incorporated in the hydrogel was varied from 0.01 g to 0.1 g in order to establish the influence of GP concentration on the dye adsorption properties of the composite. Notably, the adsorption percentage for MG increased from 76 to 89 % as the amount of GP

increased from 0.01 g to 0.1 g, the maximum MG removal percentage was observed when 0.05g of GP added into the hydrogel (**Figure 7a**). Without GP, the adsorption percentage of NaA-cl-AAc hydrogel was 65.8 % which have shown the significant role of GP in enhancing MG removal. In particular, the adsorption efficiency of the hydrogel was significantly lower than that of the hydrogel composite due to the incorporation of graphite [46,47]. In addition, GP has negative charge potential and coupling it with the hydrogel increases the anionic moieties of the hydrogel composite. Hence, the adsorption becomes more favourable due to the strong surface charge differences. However, beyond 0.05 g GP, there was no remarkable change in the adsorption percentage of MG dye. Therefore, the sample containing 0.05 g of GP was identified as the best material towards MG removal and was used to optimise the other experimental parameters.

4.2. Effect of pH on MG adsorption

pH is one of the most important parameter in dye adsorption, as it influences the dye speciation, adsorbent ability and surface charge, which overall determine the dye-pollutant interactions. To understand the influence of pH, batch experiments were carried out under controlled conditions while varying the pH from 1 to 8 (**Figure 7b**). It was noted that the adsorption percentage increased with the pH from pH 1 to 7, where it reached a maximum value of 89.71%. Typically, at low pH (1 to 3), there is high concentration of H^+ ions which compete with the cationic dye species for the active sites in the hydrogel composite, which effectively decrease the dye adsorption efficiency. Furthermore, at low pH, the adsorbent is largely positively charged which causes strong repulsive forces towards the positively charged dye species. After increasing the pH value from 3 to 6, the concentration of the H^+ ions and the positive charge on the hydrogel composite get reduced [48]. This results in a significant improvement in the removal of the dye molecules. Particularly, maximum dye adsorption was observed at pH 7 (89.71 %) due to the electrostatic attractions between the

predominantly positively charged dye species and negatively charged hydrogel composite. Thus, pH 7 was selected as optimum pH for further adsorption experiments. In addition, the adsorbent material contains some chelating groups like sulfonic acid, carboxylic and hydroxyl ions which participate in accepting and donation of protons at different pH values. Importantly, the removal efficiency of organic dyes depends upon the charge of the prepared hydrogel composite, as the anionic character increased there was an increase in strong attractive forces between the negatively charged hydrogel composite and positively charged MG dye.

4.3. Effect of adsorbent dose

The adsorbent dose was varied from 0.01 g to 0.06 g in 50 mg L^{-1} of MG aqueous solution. It could be seen in **Figure 7c** that MG removal increased from 60 % to 92 % as the adsorbent dose increased from 0.01 g to 0.04 g, where it reached its maximum. This could be linked to the provision of adequate adsorption sites and increased surface area as the amount of adsorbent increased. Also, at lower adsorbent concentrations, there was a lower spatial prohibition in the molecular structure of MG dye, resulting to increased interactions at the initial stages of the adsorption process.

4.4. Effect of initial dye concentration

Figure 7d shows the effect of initial dye concentration (50 mg L^{-1} to 500 mg L^{-1}) on the adsorption capability of NaA-cl-AAc-GP hydrogel composite. As the MG initial concentration increased from 50 ppm to 500 ppm, MG removal dropped from a maximum removal of 92 % at 50 ppm to 74 % at 500 ppm. The higher MG removal at low dye concentration could be attributed to the availability of adequate adsorption sites on the adsorbent. However, as the dye concentration increases, the adsorption sites become saturated with dye molecules, resulting to decreased uptake of the dye molecules.

4.5. Effect of contact time

The contact time is important parameter in the batch adsorption as optimization of the contact time is necessary for industrial recommendation. The contact time optimization for MG dye adsorption was examined at optimized conditions (pH = 7, adsorbent dose = 40 mg, dye concentration = 50 mg L^{-1}). The adsorption experiment for MG dye was conducted for 120 min and result is represented in the **Figure 7e**. The adsorption percentage of MG dye was sharply increased with the time up to 18 min and it reached equilibrium point after 60 min. Initially, adsorption percentage was increased sharply due to high vacant sites present in hydrogel composite and equilibrium point was reached due to saturation of the active sites in the hydrogel composite.
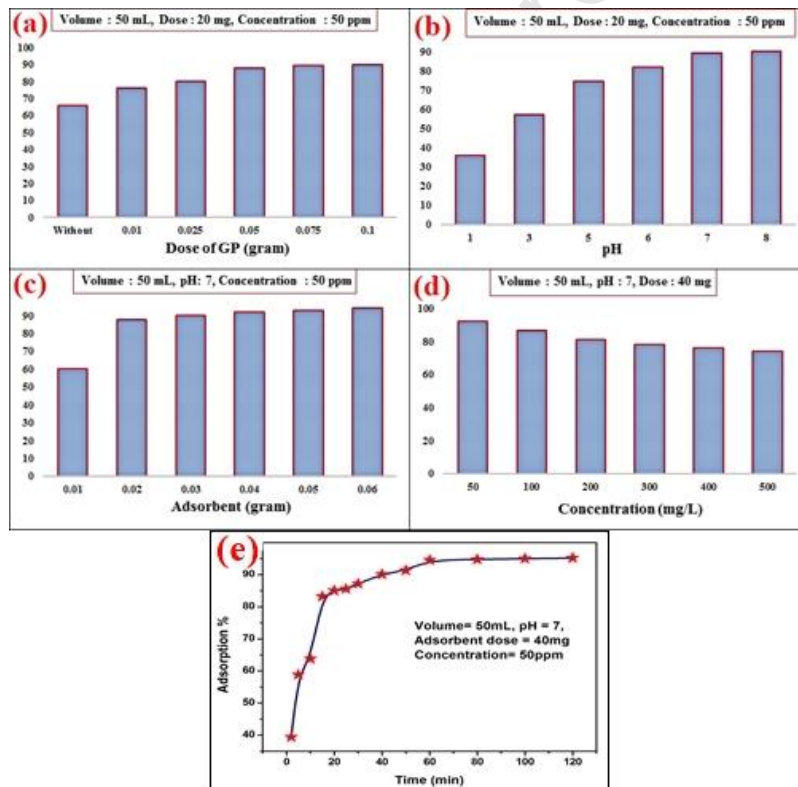

Figure 7. Effect of (a) GP dose, (b) pH, (c) adsorbent dose, (d) dye concentration and (e) contact time on the adsorption of MG dye by NaA-cl-AAc-GP hydrogel composite.

4.6. Adsorption kinetics

The influence of contact time on the adsorption performance of the NaA-cl-AAc-GP hydrogel composite at different MG dye concentration (50 and 100 mg L^{-1}) was studied as

shown in **Figure S10.** The adsorption data was analysed using kinetic models such as pseudo first-order, pseudo second-order and intra-particle diffusion models (supporting information). The MG adsorption on the hydrogel composite was better described by the pseudo second-order kinetic model, as evident from the high correlation coefficient values and smaller difference between experimental and calculated adsorption capacity compared to the pseudo first order. **Figure S10c** is a graphical representation for intra-particle diffusion and the graph is divided into two linear sections which confirm successive adsorption of MG dye onto NaA-cl-AAc-GP hydrogel composite. The first step shows the rapid adsorption of MG dye on the hydrogel composite due to the large surface area and strong electrostatic attractions. Subsequently, the second linear step is for the final equilibrium phase of adsorption. Basically, MG dye molecules were trapped into the inner pores of NaA-cl-AAc-GP hydrogel composite by intra-particle diffusion. The parameters of this kinetic study were calculated from the intercept and slope using intra-particle diffusion equation and the results are given in **Table S1**. Hence, it is concluded that both surface adsorption as well as intra-particle diffusion were responsible for the adsorption of MG dye onto NaA-cl-AAc-GP hydrogel composite.

4.7. Adsorption isotherms

The adsorption isotherms are important in adsorptive dye removal applications because they explain the interactions between the absorbent and adsorbate species. In order to determine the equilibrium adsorption capacity of NaA-cl-AAc-GP hydrogel composite for MG dye, the equilibrium isotherm was measured at three different temperatures (25 °C, 35 °C and 45 °C) as shown in the **Figure S11**. Subsequently, the adsorption isotherm data was analysed using Langmuir and Freundlich isotherm models (supporting information).High R^2 values for the Langmuir isotherm indicate that the experimental data best fitted the Langmuir isotherm model compared to the Freundlich isotherm model. Therefore, MG dye adsorbed as a

monolayer on the NaA-cl-AAc-GP hydrogel composite surface. Accordingly, the maximum MG adsorption capacity by the NaA-cl-AAc-GP hydrogel composite was calculated to be 628.93 mg g^{-1} at 35 °C **(Table S2)**.

5. Adsorption-desorption study

Adsorption-desorption tendency is an important parameter for an adsorbent because it directly affects the adsorption efficiency. It also plays important role in both ecological and economic point of view. So, we studied adsorption-desorption rate of the NaA-cl-AAc-GP hydrogel composite for five times. The recyclability of NaA-cl-AAc-GP hydrogel composite was examined using 0.1N HCl as desorbing agent and 0.1N NaOH as regenerating agent and then was washed with distilled water for further use. The MG dye concentration of 50 mg L^{-1} was used for adsorption-desorption study. As shown in **Figure S12**, the maximum adsorption percentage are 97.58 % in 1st cycle, 94.67 % in 2nd cycle, 91.89 % in 3rd cycle and 79.63 % after 5th cycle for NaA-cl-AAc-GP hydrogel composite. These results suggest good reusability of NaA-cl-AAc-GP hydrogel composite for removal of MG dye from aqueous solution by using normal reconditioning agents.

6. Comparison of the adsorption capacity of the NaA-cl-AAc-GP hydrogel composite with other adsorbents for MG dye

The comparison between the adsorption capacities of previously reported composites with the present work is presented in the **Table S3**. Remarkably, the prepared NaA-cl-AAc-GP hydrogel composite showed significantly higher MG adsorption capacity compared to nine different adsorbents reported in the literature. This could be linked to the presence of many functional groups like carboxylic groups and hydroxyl groups which are able to interact with the cationic MG dye by electrostatic interactions and hydrogen bonding, thereby enhancing MG removal. Since NaA was used as a backbone and GP as a filler, this makes the NaA-cl-AAc-GP hydrogel composite environmental friendly, biodegradable and cost-effective.

7. Conclusion

In this study, we reported the successful preparation of NaA-cl-AAc-GP hydrogel composite using radical co-polymerization method. The crystalline allotropic form of carbon, graphite, having unique thermal properties could be easily trapped inside the hydrogel matrix. Moreover, the prepared NaA-cl-AAc-GP hydrogel composite showed effective adsorption for malachite green dye. Analysis of the adsorption data revealed that the pseudo second-order adsorption kinetic model and Langmuir isotherm model best described the adsorption of MG dye onto hydrogel composite. The maximum adsorption tendency from Langmuir model was calculated to be 628.93 mg g^{-1}. High adsorption capability of the prepared composite is mainly due to distinctive surface morphology, large surface area and strong functional groups which provide desirable sites for the surface assimilation of organic dye. Thus, graphite integrated hydrogel composite may serve as potential adsorbent for the adsorption of organic pollutants from waste water.

Acknowledgments

References

[1] S. Thakur, J. Chaudhary, V. Kumar, V.K. Thakur, Progress in pectin based hydrogels for water purification: Trends and challenges, Journal of Environmental Management. 238 (2019) 210–223.

[2] R. Malik, D.S. Ramteke, S.R. Wate, Adsorption of malachite green on groundnut shell waste based powdered activated carbon, Waste Management. 27 (2007) 1129–1138.

[3]   S. Thakur, B. Sharma, A. Verma, J. Chaudhary, S. Tamulevicius, V.K. Thakur, Recent approaches in guar gum hydrogel synthesis for water purification, International Journal of Polymer Analysis and Characterization. 23 (2018) 621–632.

[4]   N. Pandey, S.K. Shukla, N.B. Singh, Water purification by polymer nanocomposites: an overview, Nanocomposites. 3 (2017) 47–66.

[5]   S. Thakur, A. Verma, B. Sharma, J. Chaudhary, S. Tamulevicius, V.K. Thakur, Recent developments in recycling of polystyrene based plastics, Current Opinion in Green and Sustainable Chemistry. 13 (2018) 32-38.

[6]   M.J. Zohuriaan-Mehr, K. Kabiri, Superabsorbent polymer materials: a review, Iranian Polymer Journal. 17 (2008) 451.

[7]   A.S. Adeleye, J.R. Conway, K. Garner, Y. Huang, Y. Su, A.A. Keller, Engineered nanomaterials for water treatment and remediation: costs, benefits, and applicability, Chemical Engineering Journal. 286 (2016) 640–662.

[8]   N.A. Peppas, Hydrogels and drug delivery, Current Opinion in Colloid & Interface Science. 2 (1997) 531–537.

[9]   J.-S. Yang, Y.-J. Xie, W. He, Research progress on chemical modification of alginate: A review, Carbohydrate Polymers. 84 (2011) 33–39.

[10]   S.N. Pawar, K.J. Edgar, Alginate derivatization: a review of chemistry, properties and applications, Biomaterials. 33 (2012) 3279–3305.

[11]   O.-N. Ciocoiu, G. Staikos, C. Vasile, Thermoresponsive behavior of sodium alginate grafted with poly (N-isopropylacrylamide) in aqueous media, Carbohydrate Polymers. 184 (2018) 118–126.

[12]   T. Hu, Q. Liu, T. Gao, K. Dong, G. Wei, J. Yao, Facile Preparation of Tannic Acid– Poly (vinyl alcohol)/Sodium Alginate Hydrogel Beads for Methylene Blue Removal from Simulated Solution, ACS Omega. 3 (2018) 7523–7531.

[13] S. Thakur, B. Sharma, A. Verma, J. Chaudhary, S. Tamulevicius, V.K. Thakur, Recent progress in sodium alginate based sustainable hydrogels for environmental applications, Journal of Cleaner Production. 198 (2018) 143-159.

[14] H. Hosseinzadeh, S. Ramin, Fabrication of starch-graft-poly (acrylamide)/graphene oxide/hydroxyapatite nanocomposite hydrogel adsorbent for removal of malachite green dye from aqueous solution, International Journal of Biological Macromolecules. 106 (2018) 101–115.

[15] J.S. Evans, T. Guo, Y. Sun, W. Liu, L. Peng, Z. Xu, C. Gao, S. He, Shape-controlled Tens-nanometers-thick Graphite and Worm-like Graphite through Lithographic Exfoliation, Carbon. 135 (2018) 248-252.

[16] Y. Bi, H. Wang, J. Liu, M. Wang, S. Ge, H. Zhang, S. Zhang, Preparation and oxidation resistance of SiC-coated graphite powders via microwave-assisted molten salt synthesis, Surface and Coatings Technology. 337 (2018) 217-222.

[17] R.S. Ruoff, M.D. Stoller, Y. Zhu, Exfoliation of Graphite Oxide in Propylene Carbonate and Thermal Reduction of Resulting Graphene Oxide Platelets, 2011.

[18] J. Fan, Z. Shi, M. Lian, H. Li, J. Yin, Mechanically strong graphene oxide/sodium alginate/polyacrylamide nanocomposite hydrogel with improved dye adsorption capacity, Journal of Materials Chemistry A. 1 (2013) 7433–7443.

[19] J. He, A. Cui, F. Ni, S. Deng, F. Shen, G. Yang, A novel 3D yttrium based-graphene oxide-sodium alginate hydrogel for remarkable adsorption of fluoride from water, Journal of Colloid and Interface Science. 531 (2018) 37–46.

[20] P. Bradder, S.K. Ling, S. Wang, S. Liu, Dye adsorption on layered graphite oxide, Journal of Chemical & Engineering Data. 56 (2010) 138–141.

[21] N. Daneshvar, M. Ayazloo, A.R. Khataee, M. Pourhassan, Biological decolorization of dye solution containing Malachite Green by microalgae Cosmarium sp., Bioresource Technology. 98 (2007) 1176–1182.

[22] B.S. Kaith, R. Jindal, R. Sharma, Synthesis of a Gum rosin alcohol-poly (acrylamide) based adsorbent and its application in removal of malachite green dye from waste water, RSC Advances. 5 (2015) 43092–43104.

[23] Y. Zhuang, F. Yu, H. Chen, J. Zheng, J. Ma, J. Chen, Alginate/graphene double-network nanocomposite hydrogel beads with low-swelling, enhanced mechanical properties, and enhanced adsorption capacity, Journal of Materials Chemistry A. 4 (2016) 10885–10892.

[24] H. Hosseinzadeh, K. Abdi, Efficient Removal of Methylene Blue Using a Hybrid Organic–Inorganic Hydrogel Nanocomposite Adsorbent Based on Sodium Alginate–Silicone Dioxide, Journal of Inorganic and Organometallic Polymers and Materials. 27 (2017) 1595–1612.

[25] T. Lu, T. Xiang, X.-L. Huang, C. Li, W.-F. Zhao, Q. Zhang, C.-S. Zhao, Post-crosslinking towards stimuli-responsive sodium alginate beads for the removal of dye and heavy metals, Carbohydrate Polymers. 133 (2015) 587–595.

[26] A. Stammati, C. Nebbia, I. De Angelis, A.G. Albo, M. Carletti, C. Rebecchi, F. Zampaglioni, M. Dacasto, Effects of malachite green (MG) and its major metabolite, leucomalachite green (LMG), in two human cell lines, Toxicology in Vitro. 19 (2005) 853–858.

[27] P. Arabkhani, A. Asfaram, Development of a novel three-dimensional magnetic polymer aerogel as an efficient adsorbent for malachite green removal, Journal of Hazardous Materials. 384 (2019) 121394.

[28] C.I. Idumah, A. Hassan, Emerging trends in graphene carbon based polymer nanocomposites and applications, Reviews in Chemical Engineering. 32 (2016) 223–264.

[29] A. Olad, M. Pourkhiyabi, H. Gharekhani, F. Doustdar, Semi-IPN superabsorbent nanocomposite based on sodium alginate and montmorillonite: Reaction parameters and swelling characteristics, Carbohydrate Polymers. 190 (2018) 295–306.

[30] B. Wattie, M.-J. Dumont, M. Lefsrud, Synthesis and Properties of Feather Keratin-Based Superabsorbent Hydrogels, Waste and Biomass Valorization. 9 (2018) 391–400.

[31] A.G. Corpuz, P. Pal, F. Banat, M.A. Haija, Enhanced removal of mixed metal ions from aqueous solutions using flotation by colloidal gas aphrons stabilized with sodium alginate, Separation and Purification Technology. 202 (2018) 103–110.

[32] S. Thakur, S. Pandey, O.A. Arotiba, Development of a sodium alginate-based organic/inorganic superabsorbent composite hydrogel for adsorption of methylene blue, Carbohydrate Polymers. 153 (2016) 34–46.

[33] A. Zhou, C. Zhu, W. Chen, J. Wan, T. Tao, T.C. Zhang, P. Xie, Phosphorus Recovery from Water by Lanthanum Hydroxide Embedded Interpenetrating Network Poly (Vinyl Alcohol)/Sodium Alginate Hydrogel Beads, Colloids and Surfaces A: Physicochemical and Engineering Aspects. 554 (2018) 237-244.

[34] Z. Tong, Y. Chen, Y. Liu, L. Tong, J. Chu, K. Xiao, Z. Zhou, W. Dong, X. Chu, Preparation, Characterization and Properties of Alginate/Poly (γ-glutamic acid) Composite Microparticles, Marine Drugs. 15 (2017) 91.

[35] P.M.K. Reddy, S.K. Mahammadunnisa, B. Ramaraju, B. Sreedhar, C. Subrahmanyam, Low-cost adsorbents from bio-waste for the removal of dyes from aqueous solution, Environmental Science and Pollution Research. 20 (2013) 4111–4124.

[36] A.P. Savintsev, Y.O. Gavasheli, Z.K. Kalazhokov, K.K. Kalazhokov, X-ray photoelectron spectroscopy studies of the sodium chloride surface after laser exposure, in: Journal of Physics: Conference Series, IOP Publishing, 2016: p. 012118.

[37] C. Zhang, L. Gao, S. Teo, Z. Guo, Z. Xu, S. Zhao, T. Ma, Design of a novel and highly stable lead-free Cs 2 NaBiI 6 double perovskite for photovoltaic application, Sustainable Energy & Fuels. 2 (2018) 2419–2428.

[38] Y. Tang, Y. Liu, W. Guo, T. Chen, H. Wang, S. Yu, F. Gao, Highly oxidized graphene anchored Ni (OH) 2 nanoflakes as pseudocapacitor materials for ultrahigh loading electrode with high areal specific capacitance, The Journal of Physical Chemistry C. 118 (2014) 24866–24876.

[39] M. Yi, Z. Shen, X. Zhang, S. Ma, Achieving concentrated graphene dispersions in water/acetone mixtures by the strategy of tailoring Hansen solubility parameters, Journal of Physics D: Applied Physics. 46 (2012) 025301.

[40] L.-Y. Wang, M.-J. Wang, Removal of heavy metal ions by poly (vinyl alcohol) and carboxymethyl cellulose composite hydrogels prepared by a freeze–thaw method, ACS Sustainable Chemistry & Engineering. 4 (2016) 2830–2837.

[41] R.L. White, C.M. White, H. Turgut, A. Massoud, Z.R. Tian, Comparative studies on copper adsorption by graphene oxide and functionalized graphene oxide nanoparticles, Journal of the Taiwan Institute of Chemical Engineers. 85 (2018) 18–28.

[42] V.J. Nebot, J. Armengol, J. Smets, S.F. Prieto, B. Escuder, J.F. Miravet, Molecular hydrogels from bolaform amino acid derivatives: A structure–properties study based on the thermodynamics of gel solubilization, Chemistry-A European Journal. 18 (2012) 4063–4072.

[43] A. Barhoum, L. Van Lokeren, H. Rahier, A. Dufresne, G. Van Assche, Roles of in situ surface modification in controlling the growth and crystallization of CaCO3

nanoparticles, and their dispersion in polymeric materials, Journal of Materials Science. 50 (2015) 7908–7918.

[44] L.-L. Tan, W.-J. Ong, S.-P. Chai, A.R. Mohamed, Reduced graphene oxide-TiO 2 nanocomposite as a promising visible-light-active photocatalyst for the conversion of carbon dioxide, Nanoscale Research Letters. 8 (2013) 465.

[45] D. Joseph, N. Tyagi, A. Ghimire, K.E. Geckeler, A direct route towards preparing pH-sensitive graphene nanosheets with anti-cancer activity, RSC Advances. 4 (2014) 4085–4093.

[46] D.D.L. Chung, A review of exfoliated graphite, Journal of Materials Science. 51 (2016) 554–568.

[47] D.D.L. Chung, Review graphite, Journal of Materials Science. 37 (2002) 1475–1489.

[48] Z. Chen, H. Deng, C. Chen, Y. Yang, H. Xu, Biosorption of malachite green from aqueous solutions by Pleurotus ostreatus using Taguchi method, Journal of Environmental Health Science and Engineering. 12 (2014) 63.

Author Statement

We appreciate and thank you & learned reviewers for the valued review comments. This would definitely improve the overall quality of the paper. The article has been revised according to the reviewer's comments/suggestions wherever necessary and we believe that it will meet the journal's expectations and can be accepted now. The changes/modifications made in the manuscript have been highlighted with RED color in the text.

Highlights

➢ Cross-linked polymeric hydrogel network was synthesized successfully.

➢ Graphite powder (GP) was incorporated into the NaA-cl-AAc hydrogel.

➢ The adsorption of dye depends on pH.

➢ NaA-cl-AAc/GP showed high adsorption capacity to malachite green dye.

➢ The hydrogel composite can be regenerated and reused effectively.

2020-01-16

Graphite modified sodium alginate hydrogel composite for efficient removal of malachite green dye

Verma, Ankit

Elsevier